



Cite this: *Green Chem.*, 2016, **18**, 5994

Received 17th August 2016,  
Accepted 2nd October 2016

DOI: 10.1039/c6gc02291j

www.rsc.org/greenchem

## Acetylene hydrochlorination over 13X zeolite catalysts at high temperature†

Zhijia Song,<sup>a,b</sup> Guangye Liu,<sup>a</sup> Dawei He,<sup>a,b</sup> Xiaodong Pang,<sup>c</sup> Yansi Tong,<sup>a,b</sup> Yaqi Wu,<sup>a,b</sup> Danhua Yuan,<sup>a</sup> Zhongmin Liu<sup>\*a</sup> and Yunpeng Xu<sup>\*a</sup>

**13X zeolite exhibited high catalytic activity and selectivity in acetylene hydrochlorination at high temperatures above 300 °C. The activity of 13X may be derived from its unique zeolite structure, meanwhile Na<sup>+</sup> and the active carbon deposit facilitated acetylene hydrochlorination. This finding presented a promising approach for the development of green non-mercury catalysts.**

Polyvinyl chloride (PVC), as one of the most widely used plastics, is manufactured by polymerization of the vinyl chloride monomer (VCM).<sup>1</sup> Currently, VCM is mainly produced *via* the oxychlorination of ethylene or the hydrochlorination of acetylene. In China, about 70% of VCM is produced from acetylene hydrochlorination using activated carbon (AC) supported HgCl<sub>2</sub> catalysts.<sup>2</sup> However, the facile volatility of HgCl<sub>2</sub> will cause high loss of mercury from the catalyst which limits the catalyst lifetime, and even worse, threatens the environment and human health.<sup>3</sup> Therefore, the exploration of environmentally friendly non-mercury catalysts is of great significance to acetylene hydrochlorination.

Normally, metal chlorides, such as HgCl<sub>2</sub>,<sup>4</sup> HAuCl<sub>4</sub>,<sup>5,6</sup> K<sub>2</sub>PdCl<sub>4</sub>,<sup>7</sup> BiCl<sub>3</sub>,<sup>8</sup> CuCl<sub>x</sub><sup>9</sup> *etc.*, were the active species of acetylene hydrochlorination. Hutchings and co-workers found a correlation between the standard electrode potentials of metal cations and their catalytic activities.<sup>10</sup> Consequently, lots of catalysts such as Au/AC,<sup>2,5,6,11–18</sup> Au–Bi/AC,<sup>8,19</sup> Au–Cu/AC,<sup>9,20</sup> Au–Co/AC,<sup>21</sup> Au–Pd/AC,<sup>22</sup> Au/SiO<sub>2</sub>,<sup>23</sup> Au–Bi/γ-Al<sub>2</sub>O<sub>3</sub>,<sup>8</sup> Ru/AC,<sup>24</sup> and Pd/Y<sup>25</sup> were developed, aiming at high activity and stability in acetylene hydrochlorination. Recently, it was reported that materials like SiC@N–C,<sup>26,27</sup> g-C<sub>3</sub>N<sub>4</sub>,<sup>28</sup> PSAC–N,<sup>29</sup> NCNTs,<sup>30</sup> and PANI–AC<sup>31</sup> had good performance in acetylene hydrochlorination without loading traditional active metal

components. Up to now, Au based catalysts have been believed to be the most promising green non-mercury catalyst candidates. However, high cost of gold would restrict its industrial application.

Zeolite was widely used as a catalyst in the petro-refining and petro-chemical industries.<sup>32,33</sup> Wang *et al.*<sup>25</sup> reported that zeolite Y could be used as a non-mercury catalyst support. Herein, we systematically investigated the acetylene hydrochlorination activity of faujasite (FAU) zeolite 13X without loading any active metal components. It was found that 13X zeolite showed very low activity under the conventional reaction temperature range of 150–200 °C. However, when the reaction temperature gradually increased to above 300 °C, the acetylene conversion increased to nearly 100%, and the VCM selectivity was more than 90%. To date, acetylene hydrochlorination over zeolite without loading other active metal components has not yet been mentioned. In addition, this was the first report about acetylene hydrochlorination at such high temperatures.

Performances of catalysts in acetylene hydrochlorination were evaluated in a fixed-bed micro-reactor (i.d. 10 mm). The loading amount of catalysts was 10 ml. The reactor was heated to the reaction temperature in a nitrogen atmosphere to remove water and air in the system before reaction. Then C<sub>2</sub>H<sub>2</sub> and HCl were fed through mass flowmeters to the reactor under ambient pressure. The flow rate of C<sub>2</sub>H<sub>2</sub> and HCl was 10 ml min<sup>−1</sup> and 12 ml min<sup>−1</sup>, respectively. The gas compositions were analyzed on-line by gas chromatography.

Fig. 1 and S1† show the catalytic performances of AC, γ-Al<sub>2</sub>O<sub>3</sub>, and SiO<sub>2</sub> and zeolites of Beta, MOR, ZSM-5, and 13X at a reaction temperature of 320 °C. γ-Al<sub>2</sub>O<sub>3</sub>, SiO<sub>2</sub>, MOR and ZSM-5 displayed very low catalytic activity, all of their acetylene conversions were below 10%. Zeolite Beta and AC gave the acetylene conversion of nearly 20% and 30%, respectively. However, zeolite 13X exhibited outstanding activity among the catalysts investigated, its highest acetylene conversion reached 98.5%. Meanwhile, the VCM selectivity of zeolite 13X exceeded 93.37%, which was slightly lower than that of AC, but higher than those of other catalysts. It was well known that the

<sup>a</sup>National Engineering Laboratory for Methanol to Olefins, Dalian National Laboratory for Clean Energy, Dalian Institute of Chemical Physics, Chinese Academy of Sciences, Dalian 116023, P. R. China. E-mail: liuzm@dicp.ac.cn, xuyyp@dicp.ac.cn

<sup>b</sup>University of Chinese Academy of Sciences, Beijing 100049, P. R. China

<sup>c</sup>Tianye (Group) Co., Ltd, Shihezi, Xinjiang 832000, China

† Electronic supplementary information (ESI) available. See DOI: 10.1039/c6gc02291j

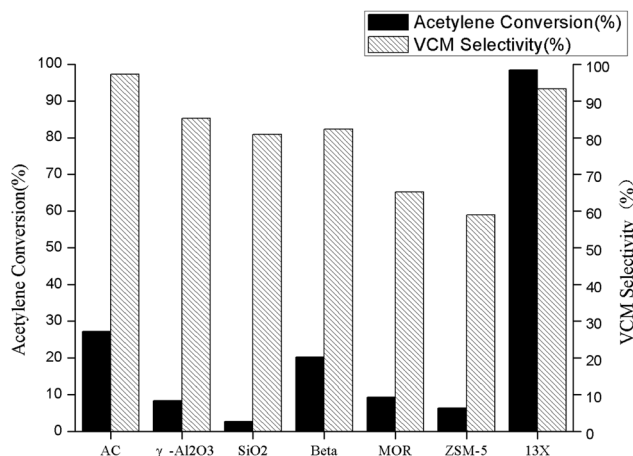


**Fig. 1** Best catalytic performances of different catalysts in acetylene hydrochlorination. Reaction conditions: reactor set point temperature = 320 °C.

reactivity of the catalyst had a close relationship with its structure and properties.<sup>26</sup> As compared to AC,  $\gamma$ -Al<sub>2</sub>O<sub>3</sub> and SiO<sub>2</sub>, zeolite 13X had a uniform microporous structure. The major difference between 13X and MOR, ZSM-5, and Beta was that 13X contained a unique supercage in its framework. Thus, it could be speculated that the remarkable acetylene hydrochlorination reactivity of 13X was ascribed to its special microporous and supercage structure.

As has been noted, AC displayed obvious acetylene hydrochlorination activity. In fact, AC was utilized as the catalyst support in most of the studies on acetylene hydrochlorination.<sup>18</sup> The detailed comparison of AC and 13X catalysts was summarized and discussed in this section (Fig. 2, S2 and S3†). When using AC as the catalyst, the acetylene conversion had a maximum value of around 40% at 220 °C, and the VCM selectivity was nearly about 99% except at 100 and 320 °C. While, the acetylene conversion of 13X increased with the temperature rising until 340 °C exhibiting an S-shaped curve, and its VCM

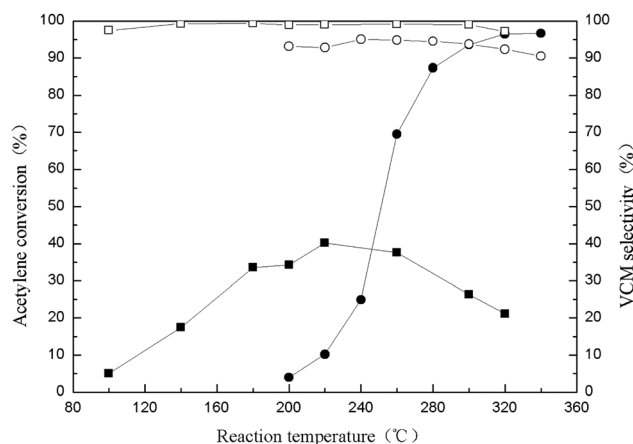


**Fig. 2** Acetylene conversion (■ AC, ●13X) and VCM selectivity (□ AC, ○13X) of catalysts at different temperatures after reacting for 2 h.

selectivity was above 90% at all temperatures. It was worth noting that the AC catalyst displayed higher activity than 13X zeolite when the reaction temperatures were below 240 °C. However, the acetylene conversion of 13X showed a sharp increase as the temperature increased above 260 °C, while that of AC decreased gradually. This result indicated that 13X exhibited unique and superior reactivity at high temperatures, which was not mentioned in previous studies.

The on-line mass spectra results are shown in Fig. 3, which revealed the variations of gas composition after feed gases passed through the catalyst bed. When AC was used as the catalyst, the reactants and the main product could be detected simultaneously after 5 min reaction. As for the 13X catalyst, the first detectable time of C<sub>2</sub>H<sub>2</sub>, VCM and HCl was 18, 40 and 62 min after reaction, respectively. Meanwhile, the breakthrough time of C<sub>2</sub>H<sub>2</sub> and HCl was 34 and 70 min, respectively (Fig. S4†). Obvious temperature rising about 16 °C in the 13X catalyst bed could be observed in the beginning of the reaction. It means that the adsorption ability of C<sub>2</sub>H<sub>2</sub>, especially HCl, on 13X was much stronger than AC. Previous studies revealed that high adsorption ability of reactants was the basic characteristic of the effective acetylene hydrochlorination catalyst.<sup>9,18,21,34,35</sup> The abundant uniform micropores, unique supercage and special basicity arising from Na<sup>+</sup> in the framework might lead to a strong adsorption of C<sub>2</sub>H<sub>2</sub> and HCl, on zeolite 13X, which was supposed to be the reason why 13X displayed higher activity than AC at high temperature.

Catalytic performances of FAU zeolites with different types of cations and different SiO<sub>2</sub>/Al<sub>2</sub>O<sub>3</sub> ratios were evaluated. Their catalytic performances and chemical compositions are shown in Fig. S5, S6 and Tables S1, S2.† The VCM selectivity of these X catalysts with SiO<sub>2</sub>/Al<sub>2</sub>O<sub>3</sub> < 3 was in the range of 91–96%, while that of Y catalysts with SiO<sub>2</sub>/Al<sub>2</sub>O<sub>3</sub> > 7 was below 70%. It indicated that the SiO<sub>2</sub>/Al<sub>2</sub>O<sub>3</sub> ratio had a great influence on VCM selectivity, and a low SiO<sub>2</sub>/Al<sub>2</sub>O<sub>3</sub> ratio was good for the FAU catalyst to catalyse the conversion of acetylene to VCM. Compared to these X catalysts with different cation types, acetylene conversion of 13X (Na-X) was more stable and much higher. Thus, it could be concluded that the cation type of X zeolite had an important effect on its catalytic activity, and Na<sup>+</sup> in the zeolite framework facilitated the conversion of acetylene. Further comparison of catalytic activities among LSX, 13X, Na-Y and Na-USY verified that high Na<sub>2</sub>O/Al<sub>2</sub>O<sub>3</sub> and low SiO<sub>2</sub>/Al<sub>2</sub>O<sub>3</sub> ratios were beneficial for acetylene conversion.

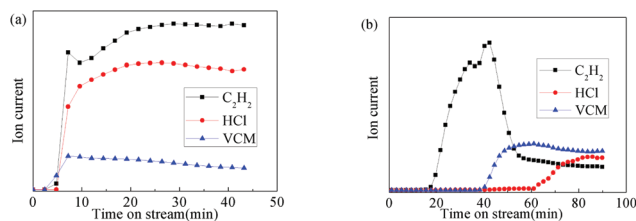


**Fig. 3** On-line mass spectrometry in the beginning of the reaction (a) AC; (b) 13X. Reaction conditions: reactor set point temperature = 320 °C.

Fig. 4 showed that acetylene conversion of the 13X catalyst decreased gradually as the reaction proceeded. The acetylene conversion decreased from 98.5% to 77.6% after 6 h. The XRD pattern of the spent 13X displayed that the crystallinity of zeolite decreased obviously as compared to the fresh catalyst (Fig. 5). Meanwhile, typical peaks of NaCl crystals could be observed in their XRD pattern. The SEM images of fresh and spent 13X catalysts showed that the catalyst was broken into irregular shape and size after deactivation (Fig. S7†). These results indicated that HCl reacted with Na<sup>+</sup> in the zeolite framework and generated NaCl crystals, which would cause the collapse of the 13X's FAU structure to some extent. Normally, carbon deposit was a predominant factor of catalyst deactivation in acetylene hydrochlorination.<sup>6</sup> TG analysis showed that the weight loss in 235–535 °C mainly is attributed to the burning of carbon deposit, so it could indicate the

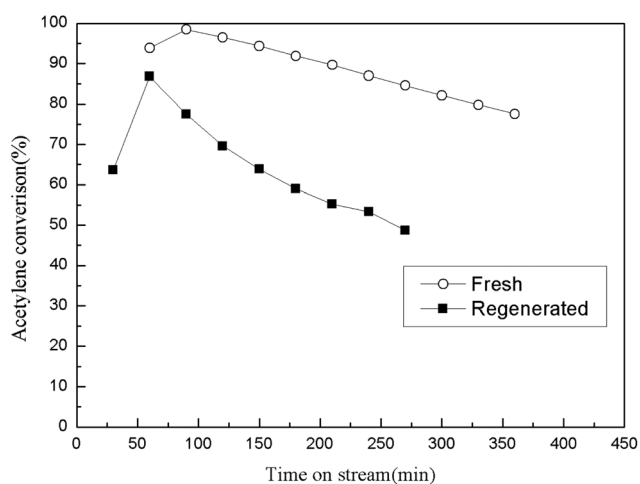


Fig. 4 Acetylene conversion of fresh and regenerated 13X catalysts. Reaction conditions: reactor set point temperature = 320 °C.

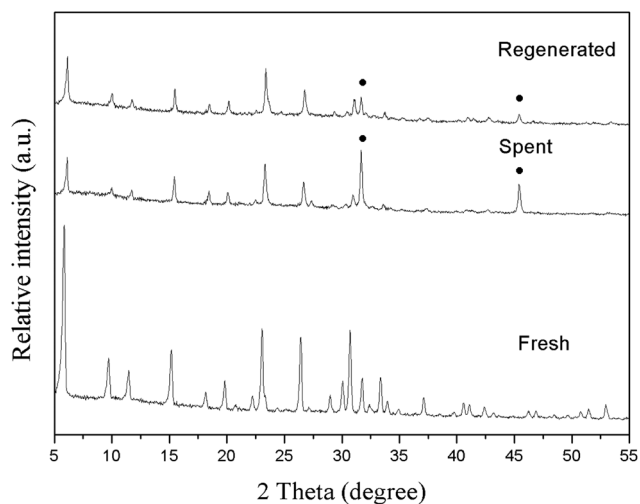


Fig. 5 XRD patterns of fresh, spent and regenerated 13X catalysts (● refers to indexed NaCl peaks).

content of carbon deposit (Fig. 6). The data in Table 1 and Fig. S8† show that the carbon deposit formed rapidly in the first 1 h reaction and then it increased slowly. The carbon deposit amount reached as high as 16.03% after 6 h. Regeneration of the catalyst was conducted by 4 h calcination in air atmosphere at 550 °C. TG analysis revealed that most of the carbon deposit on the spent catalyst could be burned off at this temperature. Although the activity of the spent catalyst was partly recovered after regeneration, the highest acetylene conversion of the regenerated catalyst was still lower than that of the fresh catalyst (Fig. S9†). The XRD pattern of the regenerated catalyst displayed that the crystallinity of zeolite slightly increased as compared to the spent catalyst. While, typical peaks of NaCl could still be observed in the regenerated catalyst though their strength decreased. Thus, it could be seen that both the collapse of the zeolite structure and the serious carbon deposit caused catalyst deactivation, while the former inhibited the completed regeneration of the spent catalyst.

An interesting phenomenon was worth noting that the catalytic activity of the 13X catalyst increased with the carbon deposit amount increasing in the beginning of the reaction (Fig. 4, Table 1 and Fig. S8†). The amount of the carbon deposit was 7.85% at 0.5 h, and increased to 9.87% at 1 h. The BET results showed that the specific surface area decreased

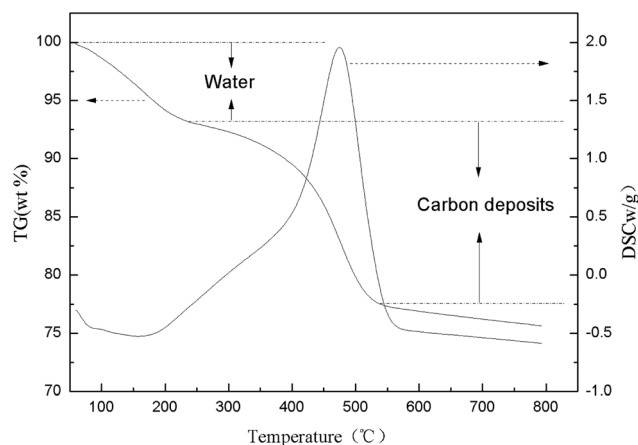


Fig. 6 TG-DSC curves of the spent catalyst (reacted 6 h). Reaction conditions: reactor set point temperature = 320 °C.

Table 1 Change of carbon deposit on catalysts as the reaction proceeded<sup>a</sup>

Reaction time (h)	Carbon deposit content <sup>b</sup> (wt %)	Carbon content <sup>c</sup> (wt %)
0.5	7.85	3.04
1	9.87	4.87
2	10.98	5.47
6	16.03	9.11

<sup>a</sup> Reaction conditions: reactor set point temperature = 320 °C. <sup>b</sup> Carbon deposit content was defined as the weight loss in the range of 235–535 °C from TGA. <sup>c</sup> Carbon content was received by TOC.

Table 2 Textural properties of catalysts

Sample	Surface area(m <sup>2</sup> g <sup>-1</sup> )	
	S <sub>BET</sub>	S <sub>micro</sub>
Fresh catalyst	501.1	461.4
Catalyst reacted 0.5 h <sup>a</sup>	171.6	110.6
Catalyst reacted 6 h <sup>a</sup>	120.7	83.7
Regenerated catalyst	249.7	173.5

<sup>a</sup> Reaction conditions: reactor set point temperature = 320 °C.

sharply from 501.1 to 171.6 m<sup>2</sup> g<sup>-1</sup> after only 0.5 h (Table 2). Normally, the serious carbon deposit and the decreasing surface area would lead to obvious deactivation of the catalyst.<sup>5</sup> However, in this experiment, the acetylene conversion of the 13X catalyst still kept increasing until 1.5 h though the carbon deposit increased. Previous research reported that carbon species could catalyse acetylene hydrochlorination effectively.<sup>26</sup> So it could be deduced that the carbon deposit on the 13X catalyst had catalytic activity and facilitated the conversion of acetylene with HCl. The <sup>13</sup>C CP/MAS NMR spectra of the spent catalyst indicated that aromatic compounds (around 130 ppm) were the main carbon deposit species (Fig. S10†). In the beginning of the reaction, the amount of the active carbon deposit increased to an optimal level, and the activity of the catalyst reached the maximum. As the reaction proceeded, the pores of the catalyst were clogged by carbon deposit gradually, and the catalyst deactivated.

In conclusion, 13X zeolite exhibited high catalytic activity in acetylene hydrochlorination at temperatures above 300 °C. The catalytic mechanism of 13X zeolite is different from the conventional metal chlorides supported catalysts. Activity of 13X may be derived from its abundant uniform micropores and unique supercage. Sodium cations in the zeolite framework and the active carbon deposit formed in the beginning of reactions could also facilitate the acetylene hydrochlorination reaction. Deactivation of 13X was caused by the collapse of its crystal structure and serious carbon deposit. The spent catalyst could be partly regenerated by calcination. This research presented a new idea for the development of acetylene hydrochlorination catalysts. Zeolite will be a promising candidate for green non-mercury catalysts.

## Acknowledgements

This work was supported by the State Key Research and Development Project of China (2016YFB0301603).

## References

- J. Zhang, N. Liu, W. Li and B. Dai, *Front. Chem. Sci. Eng.*, 2011, **5**, 514–520.
- K. Zhou, J. C. Jia, C. H. Li, H. Xu, J. Zhou, G. H. Luo and F. Wei, *Green Chem.*, 2015, **17**, 356–364.
- I. T. Trotus, T. Zimmermann and F. Schuth, *Chem. Rev.*, 2014, **114**, 1761–1782.
- G. J. Hutchings and D. T. Grady, *Appl. Catal.*, 1985, **16**, 411–415.
- B. Nkosi, M. D. Adams, N. J. Coville and G. J. Hutchings, *J. Catal.*, 1991, **128**, 378–386.
- B. Nkosi, N. J. Coville, G. J. Hutchings, M. D. Adams, J. Friedl and F. E. Wagner, *J. Catal.*, 1991, **128**, 366–377.
- T. V. Krasnyakova, I. V. Zhikharev, R. S. Mitchenko, V. I. Burkhovetski, A. M. Korduban, T. V. Kryshchuk and S. A. Mitchenko, *J. Catal.*, 2012, **288**, 33–43.
- J. G. Zhao, X. G. Cheng, L. Wang, R. F. Ren, J. J. Zeng, H. H. Yang and B. X. Shen, *Catal. Lett.*, 2014, **144**, 2191–2197.
- H. Y. Zhang, B. Dai, W. Li, X. G. Wang, J. L. Zhang, M. Y. Zhu and J. J. Gu, *J. Catal.*, 2014, **316**, 141–148.
- G. J. Hutchings, *J. Catal.*, 1985, **96**, 292–295.
- G. J. Hutchings and R. Joffe, *Appl. Catal.*, 1986, **20**, 215–218.
- G. J. Hutchings, *Catal. Today*, 2002, **72**, 11–17.
- M. Conte, C. J. Davies, D. J. Morgan, T. E. Davies, D. J. Elias, A. F. Carley, P. Johnston and G. J. Hutchings, *J. Catal.*, 2013, **297**, 128–136.
- M. Conte, C. J. Davies, D. J. Morgan, T. E. Davies, A. F. Carley, P. Johnston and G. J. Hutchings, *Catal. Sci. Technol.*, 2013, **3**, 128–134.
- M. Conte, C. J. Davies, D. J. Morgan, A. F. Carley, P. Johnston and G. J. Hutchings, *Catal. Lett.*, 2014, **144**, 1–8.
- M. Conte, A. F. Carley and G. J. Hutchings, *Catal. Lett.*, 2008, **124**, 165–167.
- M. Conte, A. F. Carley, C. Heirene, D. J. Willock, P. Johnston, A. A. Herzing, C. J. Kiely and G. J. Hutchings, *J. Catal.*, 2007, **250**, 231–239.
- P. Johnston, N. Carthey and G. J. Hutchings, *J. Am. Chem. Soc.*, 2015, **137**, 14548–14557.
- K. Zhou, W. Wang, Z. Zhao, G. H. Luo, J. T. Miller, M. S. Wong and F. Wei, *ACS Catal.*, 2014, **4**, 3112–3116.
- S. J. Wang, B. X. Shen and Q. L. Song, *Catal. Lett.*, 2010, **134**, 102–109.
- H. Y. Zhang, B. Dai, X. G. Wang, W. Li, Y. Han, J. J. Gu and J. L. Zhang, *Green Chem.*, 2013, **15**, 829–836.
- M. Conte, A. F. Carley, G. Attard, A. A. Herzing, C. J. Kiely and G. J. Hutchings, *J. Catal.*, 2008, **257**, 190–198.
- X. H. Tian, G. T. Hong, Y. Liu, B. B. Jiang and Y. R. Yang, *RSC Adv.*, 2014, **4**, 36316–36324.
- J. L. Zhang, W. Sheng, C. L. Guo and W. Li, *RSC Adv.*, 2013, **3**, 21062–21068.
- L. Wang, F. Wang, J. D. Wang, X. L. Tang, Y. L. Zhao, D. Yang, F. M. Jia and T. Hao, *React. Kinet., Mech. Catal.*, 2013, **110**, 187–194.
- X. Li, X. Pan, L. Yu, P. Ren, X. Wu, L. Sun, F. Jiao and X. Bao, *Nat. Commun.*, 2014, **5**, 3688.
- X. Y. Li, X. L. Pan and X. H. Bao, *J. Energy Chem.*, 2014, **23**, 131–135.
- X. Y. Li, Y. Wang, L. H. Kang, M. Y. Zhu and B. Dai, *J. Catal.*, 2014, **311**, 288–294.

- 29 X. G. Wang, B. Dai, Y. Wang and F. Yu, *ChemCatChem*, 2014, **6**, 2339–2344.
- 30 K. Zhou, B. Li, Q. Zhang, J. Q. Huang, G. L. Tian, J. C. Jia, M. Q. Zhao, G. H. Luo, D. S. Su and F. Wei, *ChemSusChem*, 2014, **7**, 723–728.
- 31 C. L. Zhang, L. H. Kang, M. Y. Zhu and B. Dai, *RSC Adv.*, 2015, **5**, 7461–7468.
- 32 M. E. Davis and R. F. Lobo, *Chem. Mater.*, 1992, **4**, 756–768.
- 33 T. Frising, P. Leflaive, T. Frising and P. Leflaive, *Microporous Mesoporous Mater.*, 2008, **114**, 27–63.
- 34 B. Dai, K. Chen, Y. Wang, L. H. Kang and M. Y. Zhu, *ACS Catal.*, 2015, **5**, 2541–2547.
- 35 G. B. Li, W. Li and J. L. Zhang, *Catal. Sci. Technol.*, 2016, **6**, 3230–3237.